9558 *J. Phys. Chem. A* **2002,** *106,* 9558−9562

Ab Initio and Topological Study of Interactions between $SiH_{4-n}X_n$ ($n = 0-3$, X = F and Cl) and BH_3

Shao-Wen Hu* and Xiang-Yun Wang

Department of Applied Chemistry, College of Chemistry and Molecular Engineering, Peking University, Beijing, China 100871

Received: April 28, 2002; In Final Form: August 14, 2002

Theoretically, silane and its derivatives ($SiH_{4-n}X_n$, $n = 0-3$, X = F and Cl) are found to form hydrogen-bridged complex with borane (BH_3) at gas phase. High level ab initio calculations at the MP2/aug-cc-pVTZ level show that the interaction energies (D_e) between $SiH_{4-n}X_n$ and BH_3 are $-6.43 \sim -12.06$ kcal/mol corrected by zero-point energy and the basis set superposition error, whereas without the corrections, the D_e values are $-14.73 \sim -21.65$ kcal/mol. The $SiH_{4-n}X_n-BH_3$ complexes can be regarded as analogues of B_2H_6 with one monomer BH_3 replaced by $SiH_{4-n}X_n$ although only one bridged bond Si−H−B is definitely located via topological analyses of the electron density. Upon bonding, boron becomes four coordinated by receiving a hydrogen atom from $SiH_{4-n}X_n$. In contrast to the compact hydrogen-bridged complexes, the electron donor−acceptor conformers with a bridged halogen atom are only loosely bound ($D_e < 2$ kcal/mol). The results indicate that BH_3 is a better hydrogen attractor in these interactions. The predicted $SiH_{4-n}X_n-BH_3$ complexation and hydrogen transfer from $SiH_{4-n}X_n$ to BH_3 may help to understand the initial stage reactions in producing boron doped silicon films by chemical vapor deposition.

I. Introduction

Silane and its halogen derivatives $SiH_{4-n}X_n$ are widely used as source gases in CVD fabricating silicon films.[1−7] It has long been observed that B_2H_6, a p-type dopant, mixed with $SiH_{4-n}X_n$ can catalyze the deposition. Boron doping efficiency and the rate of film deposition are greatly influenced by variation of the B_2H_6 concentration and the species of $SiH_{4-n}X_n$.[8−12] Under CVD conditions, decomposition and recombination of source gas molecules may happen at several stages. The system is further complicated by surface absorption and desorption.[13−15] The actual experimental condition is thus crucial and can be adjusted to control dominant reactions at certain stage. Initially, B_2H_6 can decompose at lower temperature than the other species.[16,17] Recently, it is found that BH_3, a possible decomposition product of B_2H_6, can theoretically form a hydrogen-bridged complex with SiH_4.[18] The geometrical and electronic structures of the SiH_4-BH_3 complex exhibit some characters of B_2H_6. As a substituent of SiH_4, SiH_2Cl_2 is able to enhance boron-doping efficiency significantly,[12] suggesting a stronger interaction between SiH_2Cl_2 and BH_3. It should be noticed that the $SiH_{4-n}X_n-BH_3$ complexes with $n = 1-3$ may have two major isomers. One is a hydrogen-bridged conformer, similar to the SiH_4-BH_3 complex. The other is a halogen-bridged conformer, with halogens as electron donors to electron deficient BH_3. With the hope that high level ab initio calculations would reveal which conformers are favored energetically and provide insight into bonding natures in addition to the geometric and electronic structures, we performed a computational research on the combining systems of $SiH_{4-n}X_n$ and BH_3.

II. Calculation Method

The previous work[18] showed that the geometry structures of SiH_4-BH_3 are completely different with and without electron correlation treatment during optimization. The optimized structural parameters, however, vary only slightly for different post SCF calculations. To facilitate the comparison between systems of various sizes, all of the geometry structures were fully optimized at the MP2/6-31+G* level. Frequency calculations at this level followed to obtain the ZPE and to testify the genuine minima. Interaction energies, defined as total electronic energy difference between $SiH_{4-n}X_n-BH_3$ complexes and the sum of monomers $SiH_{4-n}X_n$ and BH_3, were obtained through single-point calculations up to the MP2/aug-cc-pVTZ level. The counterpoise method[19] was used to evaluate the basis sets superposition errors (BSSE). The Guassian 98 program package[20] was employed for these calculations.

Wave functions obtained at the MP2/6-31+G* level are used for the topological analyses of the electron densities. The electronic structures are visualized as contour maps of electron density overlaid with its gradient trajectories. The AIM2000 program[21] derived from Bader's "atoms in molecules" (AIM) theory[22] was employed for these purposes.

III. Results and Discussions

To our knowledge, the $SiH_{4-n}X_n-BH_3$ complexes, though simple and important, have not been subjected to any theoretical or experimental investigations.[23,24] The results and discussions about the $SiH_{4-n}X_n-BH_3$ complexes obtained in this work are, therefore, intentionally compared with the more familiar borane adducts B_2H_6,[25−28] $B_2H_7^-$,[29−31] and NH_3-BH_3,[32−38] in a sense that the hydrogen-bridged conformers are analogues of B_2H_6 or $B_2H_7^-$ with one BH_3 or BH_4^- replaced by a $SiH_{4-n}X_n$, whereas the halogen-bridged conformers are analogues of the NH_3-BH_3 with the electron donor NH_3 replaced by a $SiH_{4-n}X_n$. Such comparisons are also motivated by the desire to understand the possible gas-phase reactions between $SiH_{4-n}X_n$ and B_2H_6 as they are both involved in the initial stage of CVD processes.

---

* To whom correspondence should be addressed. E-mail: swhu@yahoo.com.

10.1021/jp0260292 CCC: $22.00 © 2002 American Chemical Society
Published on Web 09/19/2002

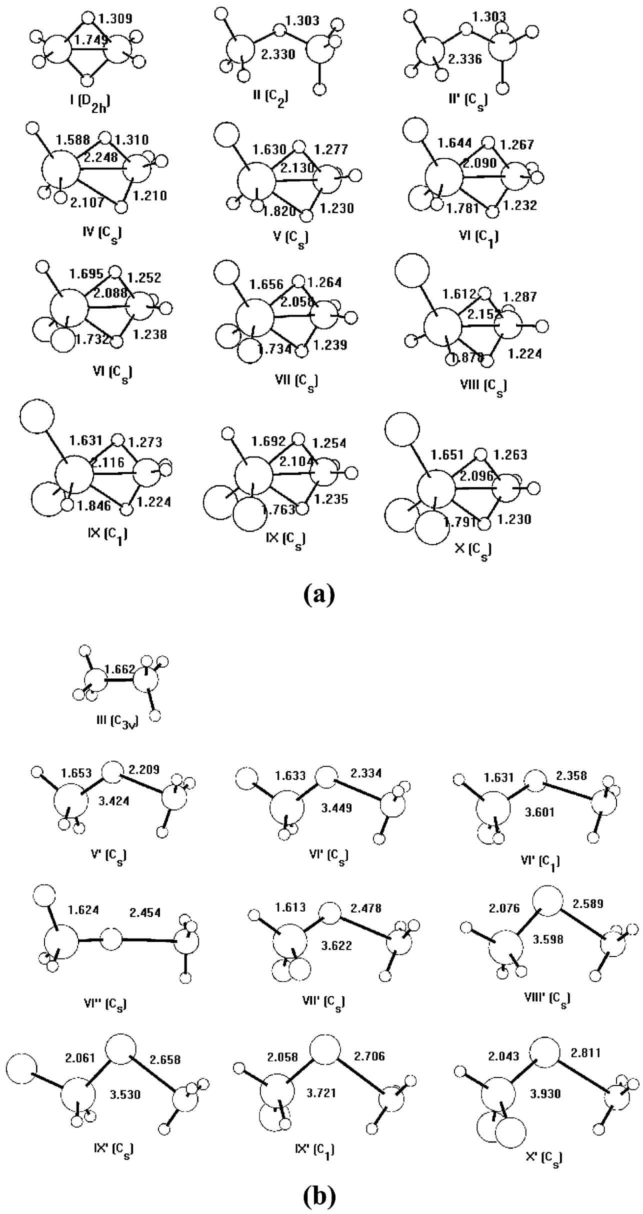

(a)

(b)

Figure 1. Optimized (MP2/6-31+G*) geometry structures of B_2H_6 (I), $B_2H_7^-$ (II), and hydrogen-bridged $SiH_{4-n}X_n-BH_3$ (IV−X) (a); NH_3-BH_3 (III) and halogen-bridged $SiH_{4-n}X_n-BH_3$ (IV′−X′) (b). Bond lengths are in angstroms. The distances of Si−H, Si−F, and Si−Cl in free $SiH_{4-n}X_n$ are 1.458−1.481, 1.605−1.637, and 2.032−2.060 Å respectively.

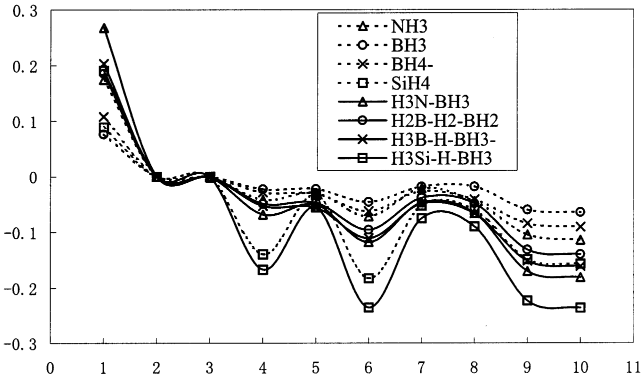

Figure 2. Theoretical model and basis set effects on the relative electronic energies of the monomers and complexes. The vertical axis is the electronic energy in a.u. (using MP2/6-31+G* optimized structures) relative to those calculated at the MP2/6-31+G* level. The horizontal axis stands for the theoretical models (1 HF and 2−10 MP2) and basis sets as, 1. 6-31+G*; 2. 6-31+G*; 3. 6-31++G*; 4. 6-311+G*; 5. 6-31+G**; 6. 6-311++G**; 7. cc-pVDZ; 8. aug-cc-pVDZ; 9. cc-pVTZ; and 10. aug-cc-pVTZ.

A. Geometries and Energies. The optimized geometry structures of $SiH_{4-n}X_n-BH_3$ complexes are shown in Figure 1, (IV to X). These structures are genuine minima except for the II′(C_s), VI(C_s), and VII(C_s) in (a) and V′(C_s), VIII′(C_s) and X′(C_s) in (b), which are saddle points with one imaginary frequency. In the hydrogen-bridged conformers (Figure 1a), the two monomers $SiH_{4-n}X_n$ and BH_3 are connected compactly. The H−B distance in Si−H−B is shorter than that appears in B_2H_6 (I) and $B_2H_7^-$ (II) for $SiH_{4-n}X_n-BH_3$ ($n = 1-3$), whereas the Si−H distance in Si−H−B is considerably longer than the Si−H bond in free $SiH_{4-n}X_n$ (1.458−1.481) Å. This hydrogen-transfer effect results in a drastic geometric change of boron from three-coordinated planar to four-coordinated distorted tetrahedral. The H in Si−H−B is slightly drawn to Si when a halogen atom is near its position. This can be understood that the electron-deficient H in Si−H−B is attracted by the electron-rich halogen. The distance and the orientation of another H in the same plane defined by Si−H−B show some back-donation characters toward $SiH_{4-n}X_n$. The Si···H distance is shorter for halogen-substituted complexes than for simple SiH_4-BH_3. The calculated structures of B_2H_6 and $B_2H_7^-$ at this level are consistent well with experiments[28,30] and earlier theoretical results.[29,31,34] It seems that the $SiH_{4-n}X_n-BH_3$ complexes are structurally more like the double hydrogen-bridged B_2H_6 rather than the mono hydrogen-bridged anion $B_2H_7^-$, and the characteristic is more evident for halogen derivatives than for the simple SiH_4-BH_3.

In the halogen-bridged conformers (Figure 1b), on the other hand, the two monomers are loosely connected. Compared with the nitrogen in the typical donor−acceptor complex H_3NBH_3 (III), halogens are much weaker electron donors. The halogen-bridged $SiH_{4-n}X_n-BH_3$ complexes are thus usual van der Waals contact, and both monomers are essentially in their original structures. It is still remarkable, however, that most of the structures prefer a bent to a linear Si−X···B configuration, indicating the probable attraction between silicon and boron or silicon and a hydrogen atom from BH_3.

To select a proper method for energetic calculations, different theoretical models and basis sets are tested for NH_3-BH_3, B_2H_6, $B_2H_7^-$, SiH_4-BH_3, and the monomers involved (Figure 2). It can be seen that, within the framework of the MP2 model, incorporating triple split basis functions is important to lower the total energies of the species containing silicon. Thus, these kinds of basis sets are chosen for evaluating the total electronic energies and are compared with the results obtained using double split basis sets (Table 1). The stabilities of the $SiH_{4-n}X_n-BH_3$ complexes are assessed by interaction energies (denoted as D_e). The calculated values of D_e using different theoretical models and basis sets are summarized in Table 2. It can be seen that including electron correlation treatment lowers the energies 12−24 kcal/mol for the hydrogen-bridged complexes (Table 2). As a result, these $SiH_{4-n}X_n-BH_3$ complexes are essentially not bonded within the limit of SCF calculations. The structures shown in Figure 1a (IV-X) fall apart when optimized at the HF/6-31+G* level. For B_2H_6, $B_2H_7^-$, and H_3NBH_3, including electron correlation is also a fundamental requirement to obtain structures and energies consistent with the experiment.[28,31,32] In the case of the halogen-bridged conformers, the electron correlation effect is considerably smaller. Some of the species have negative interaction energies at the SCF level.

TABLE 1: Calculated Total Electronic Energies *E* and ZPE of $SiH_{4-n}X_n-BH_3$[a]

		E^b		ZPE[c]			E^b		ZPE[c]
H		6-311++g**	aug-cc-pVTZ	6-31+g*	X		6-311++g**	aug-cc-pVTZ	6-31+g*
IV(C_s)	$H_3Si-H-BH_3$	−318.02408	−318.02511	41.73 (0)					
V(C_s)	$FH_2Si-H-BH_3$	−417.20063	−417.26551	39.49 (0)	V′(C_s)	$H_3Si-F-BH_3$	−417.18327	−417.23951	36.58 (1)
VI(C_1)	$F_2HSi-H-BH_3$	−516.37250	−516.50172	36.08 (0)	VI′(C_s)	$FH_2Si-F-BH_3$	−516.35758	−516.47761	33.37 (0)
VI(C_s)	$F_2HSi-H-BH_3$	−516.36968	−516.49952	35.92 (1)	VI′(C_1)	$FH_2Si-F-BH_3$	−516.35775	−516.47687	33.30 (0)
					VI″(C_s)	$FH_2Si-F-BH_3$	−516.35693	−516.47585	33.03 (0)
VII(C_s)	$F_3Si-H-BH_3$	−615.54539		32.39 (1)	VII′(C_s)	$F_2HSi-F-BH_3$	−615.53432		29.72 (0)
VIII(C_s)	$ClH_2Si-H-BH_3$	−777.18594		38.67 (0)	VIII′(C_s)	$H_3Si-Cl-BH_3$	−777.17199		35.98 (1)
IX(C_1)	$Cl_2HSi-H-BH_3$	−1236.34126		34.53 (0)	IX′(C_s)	$ClH_2Si-Cl-BH_3$	−1236.32865		32.13 (0)
IX(C_s)	$Cl_2HSi-H-BH_3$	−1236.34012		34.55 (0)	IX′(C_1)	$ClH_2Si-Cl-BH_3$	-1236.32904		32.05 (0)
X(C_s)	$Cl_3Si-H-BH_3$	−1695.49699		30.21 (0)	X′(C_s)	$Cl_2HSi-Cl-BH_3$	-1695.48595		27.61 (1)

[a] Single-point calculation using the MP2/6-31+G* optimized geometry structures. [b] Total electronic energies are in atomic units (au). [c] Zero-point energies are in kcal/mol. The numbers of imaginary frequencies are in parentheses.

TABLE 2: Interaction Energies of B_2H_6, $B_2H_7^-$, NH_3-BH_3, and $SiH_{4-n}X_n$-BH_3[a]

	D_e (HF)	D_e (MP2)					CPC[c]			
	I	I	II	III	IV	ZPEC[b]	D	A	D_e(CC)[d]	D(exp)[e]
					H					
I(D_{2h})	−19.75	−40.36	−43.01	−47.80	−47.30	6.89	1.94	1.94	−36.52	−25 ~ −60
II(C_2)	−22.98	−34.84	−36.75	−39.44	−38.67	4.58	1.87	1.08	−31.15	−31 ± 8
II′(C_s)	−23.00	−34.80	−36.71	−39.39	−38.66	4.44	1.91	1.05	−31.27	
IV(C_s)	10.70	−5.14	−9.62	−13.98	−14.73	4.39	2.75	1.16	−6.43	
V(C_s)	7.65	−10.62	−15.47	−20.96	−21.65	4.71	3.45	1.42	−12.06	
VI(C_1)	10.96	−8.15	−12.83	−18.92	−19.29	4.29	4.00	1.54	−9.46	
VI(C_s)	13.45	−6.26	−11.06	−17.31	−17.91	4.12	4.37	1.58	−7.84	
VII(C_s)	14.89	−4.42	−9.49	−15.70	4.00	4.76	1.76			
VIII(C_s)	10.14	−8.46	−13.77		4.54	4.23	1.36			
IX(C_1)	14.72	−6.54	−12.16		4.13	5.82	1.45			
IX(C_s)	16.72	−5.63	−11.45		4.16	6.92	1.53			
X(C_s)	18.85	−4.70	−10.61		3.99	7.94	1.55			
					X					
III(C_{3v})	−21.59	−32.14	−32.43	−35.69	−33.61	5.84	3.55	1.04	−23.18	−31.1
V′(C_s)	−0.72	−4.00	−4.57		−5.34	1.80	1.51	0.48	−1.54	
VI′(C_s)	−0.69	−3.00	−3.47		−4.16	1.58	1.16	0.44	−0.98	
VI′(C_1)	−0.68	−3.14	−3.57		−3.70	1.50	1.12	0.44	−0.64	
VI″(C_s)	−1.35	−3.00	−3.06		−3.05	1.23	0.74	0.44	−0.64	
VII′(C_s)	−0.26	−2.38	−2.55			1.32	0.97	0.41		
VIII′(C_s)	1.49	−3.77	−5.01			1.85	2.58	0.36		
IX′(C_s)	1.39	−3.26	−4.25			1.73	2.48	0.37		
IX′(C_1)	1.57	−3.36	−4.49			1.66	2.46	0.35		
X′(C_s)	1.34	−2.77	−3.68			1.39	2.35	0.34		

[a] Interaction energies D_e (kcal/mol) calculated at different levels using the MP2/6-31+G* optimized geometries. The basis sets employed are 6-31+G* (I), 6-311++G** (II), cc-pVTZ (III), and aug-cc-pVTZ (IV). See Table 1 for the species and Figure 1 for the structures. [b] Zero-point energy corrections ZPEC (kcal/mol) calculated at the MP2/6-31+G* level. [c] Counterpoise corrections CPC (kcal/mol) for hydrogen or electron donor (D) and acceptor (A) calculated at the MP2/6-311++G** level. [d] Interaction energies with approximate (smaller basis sets) ZPE and BSSE corrections, $D_e(CC) = D_e + ZPEC^b + CPC^c$. [e] Experimental estimation of enthalpy change (kcal/mol) from refs 27, 29, and 33.

Counterpoise (CP) methods[19] were used in BSSE corrections for interaction energies. Because the interactions of the borane adducts involve large amount of charge-transfer components,[37] the species studied here can be regarded as electron donor−acceptor complexes with BH_3, BH_4^-, NH_3, and $SiH_{4-n}X_n$ as donors, and BH_3 as the acceptor, respectively. The full CP corrections for the complexes are the sum of the CP corrections for the donors and acceptors, which are energy difference between donor (acceptor) with and without the acceptor's (donor's) basis sets. Both donor and acceptor are at the geometry of the fragments in the optimized complex. It can be seen (Table 2) that the corrections are significant especially for the donors, and the values seem to reduce quite slow as the basis sets turns larger (not shown). Controversy remains on the problem of overcorrection if ZPE and BSSE are both included in the final report of interaction energy.[39−42] Experimentally, the large discrepancy of the dissociation energies also exists for the known borane adducts B_2H_6,[27] $B_2H_7^-$,[29] and NH_3BH_3.[33] It is, therefore, more reliable to give upper and lower limits of the interaction energy and to speak of the stabilities of the $SiH_{4-n}X_n-BH_3$ complex as relative to B_2H_6, $B_2H_7^-$, and NH_3BH_3. Because incorporating large basis sets is computationally difficult for species containing chlorine, the finial MP2/aug-cc-pVTZ results for these species can be estimated from the relative values obtained at the MP2/6-311++G** level.

Among the $SiH_{4-n}X_n-BH_3$ complexes, $H_2FSi-H-BH_3$ (V (*C*$_s$)) has the largest interaction energy (−12.06 to −21.65 kcal/mol). The values are about 33−46% the energy needed to dissociate B_2H_6 into BH_3. Thus, B_2H_6 dissociation may be driven by the formation of the $SiH_{4-n}X_n-BH_3$ complexes. It can be seen from geometries (Figure 1) and interaction energies (Table 2) that the halogen derivatives are all better stabilizers to BH_3 relative to SiH_4. When substituting SiH_4 in the CVD experiment, the higher bonding tendency of the $SiH_{4-n}X_n$ (with $n = 1{\sim}3$) toward BH_3 probably promotes the observed variations in boron-doping efficiency and other properties.

B. Topological Properties and Bonding Nature. In B_2H_6, there are 12 valence electrons shared by four terminal B−H and two bridged B−H−B bonds. The B−H−B bonds are thus three-center−two-electron bonds and each boron atom is four

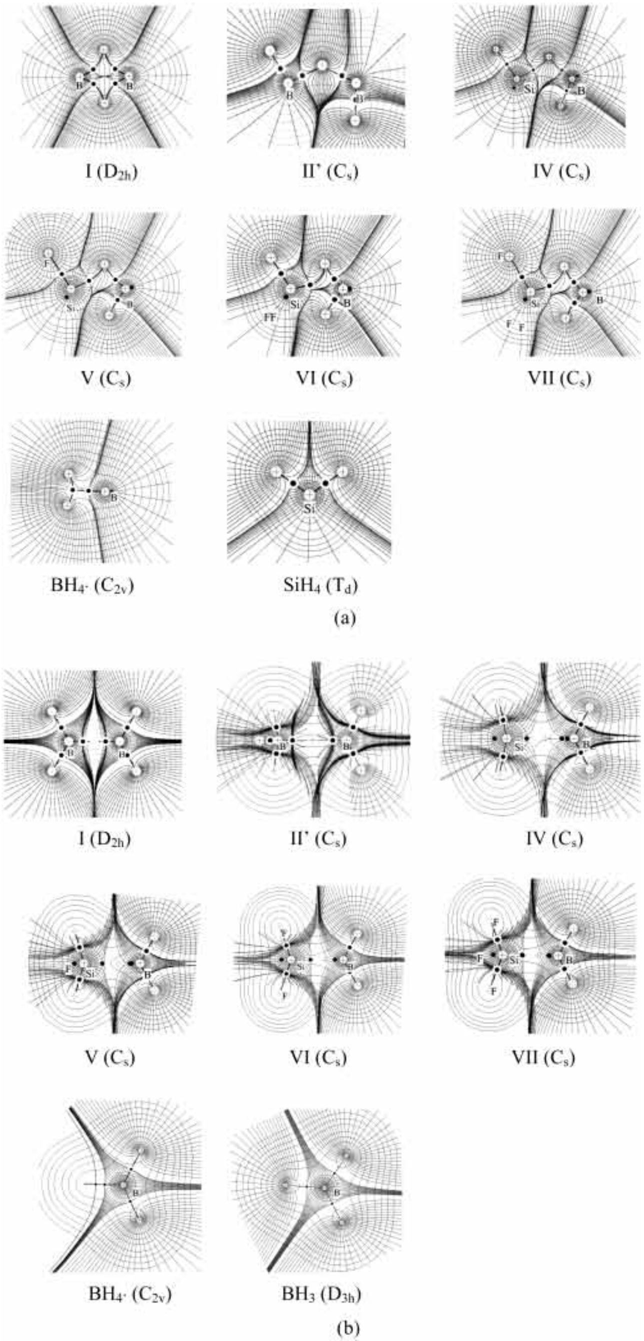

Figure 3. Contour map of electron density overlaid with gradient trajectories of $\nabla\rho$ for B_2H_6, $B_2H_7^-$, $BH_4^\bullet$, SiH_4, BH_3, and selected $SiH_{4-n}X_n-BH_3$ complexes. Crosses represent nuclei positions while black circles represent BCP. (a) Projection on the plane defined by bridged-hydrogen, silicon (boron), and boron. (b) Projection on the plane perpendicular to the plane in (a) and contains silicon (boron) and boron.

TABLE 3: Electron Density ρ_c, Laplacian $\nabla^2\rho_c$, and Ellipticity ϵ of Selected BCP in B_2H_6, $B_2H_7^-$, and $SiH_{4-n}X_n-BH_3$ Complexes[a]

		Si(B)−H−B		B−H3		
		Si(B)−H	H−B	B−H(b)[b]	B−H(2)	B−H(3)
ρ_c	I(D_{2h})	0.128	0.128	0.128	0.183	0.183
	II(C_2)	0.105	0.105	0.159	0.165	0.162
	IV(C_s)	0.089	0.105	0.163	0.174	0.174
	V(C_s)	0.086	0.121	0.149	0.176	0.176
	VI(C_s)	0.085	0.133	0.142	0.176	0.176
	VII(C_s)	0.092	0.128	0.143	0.178	0.178
	IX(C_1)	0.090	0.122	0.152	0.175	0.176
	IX(C_s)	0.083	0.132	0.143	0.176	0.176
$\nabla^2\rho_c$	I(D_{2h})	−0.004	−0.004	−0.004	−0.427	−0.427
	II(C_2)	0.045	0.045	−0.267	−0.253	−0.245
	IV(C_s)	0.108	0.154	−0.223	−0.336	−0.336
	V(C_s)	0.100	0.109	−0.091	−0.361	−0.361
	VI(C_s)	0.033	0.052	−0.018	−0.362	−0.362
	VII(C_s)	0.055	0.086	−0.028	−0.381	−0.381
	IX(C_1)	0.083	0.115	−0.106	−0.354	−0.367
	IX(C_s)	0.040	0.017	−0.030	−0.340	−0.340
ϵ	I(D_{2h})	1.122	1.122	1.122	0.076	0.076
	II(C_2)	0.192	0.192	0.114	0.116	0.105
	IV(C_s)	0.379	0.112	0.003	0.089	0.089
	V(C_s)	0.763	0.148	0.026	0.041	0.041
	VI(C_s)	4.724	0.057	0.029	0.010	0.010
	VII(C_s)	2.158	0.075	0.005	0.018	0.018
	IX(C_1)	0.883	0.191	0.066	0.043	0.039
	IX(C_s)	3.257	0.034	0.002	0.022	0.022

[a] The values of BCP for Si−H in SiH_4 are $\rho_c = 0.117$, $\nabla^2\rho_c = 0.159$, $\epsilon = 0$; for B−H in BH_3, they are $\rho_c = 0.184$, $\nabla^2\rho_c = -0.451$, $\epsilon = 0.283$. [b] The partial bridged bond in the $SiH_{4-n}X_n-BH_3$ complexes.

coordinated. With one more negative hydrogen ion, $B_2H_7^-$ has 14 valence electrons shared by six pairs of terminal B−H bonds and one pair of electrons belong to the B−H−B bond so as to satisfy the four coordination of both boron atoms. The $SiH_{4-n}X_n-BH_3$ complex has also 14 valence electrons and seven hydrogen atoms. It is, however, questionable that the electrons are distributed in a same way as $B_2H_7^-$. Geometrically (Figure 1a), two hydrogen atoms appear in the same plane with silicon and boron between them. Compared with boron, silicon is more likely to form bonds beyond four because it has more nuclear charge and empty 3d orbitals. To understand the bonding nature, we performed topological analyses of electron density. Our calculations show that no bond critical points (BCP) exist between silicon and boron or silicon and another hydrogen. This additional bond is thus not formed according to the criterion provided by the AIM theory. The contour diagrams of electron density overlaid by the gradient trajectories of several $SiH_{4-n}F_n-BH_3$ complexes are depicted along with B_2H_6 and $B_2H_7^-$ in Figure 3. The maps of the $SiH_{4-n}Cl_n-BH_3$ complexes are similar to their fluorine counterparts and are omitted. Examining the atomic basins defined by surfaces with zero flux of gradient trajectory, we can see that the atoms around silicon resemble $B_2H_7^-$ of C_s symmetry, whereas the atoms around boron resemble B_2H_6. The later resemblance, more significant for halogen-substituted complexes than simple SiH_4-BH_3, originated from the attraction between silicon and the partially bridged hydrogen atom. It is interesting to note that the electronic structures of the boron part in the $SiH_{4-n}X_n-BH_3$ complexes bare some similarities to that of the $BH_4^\bullet$ radical. Probably one of the subsequent reactions of the $SiH_{4-n}X_n-BH_3$ complexes in the CVD process would involve such a radical. The contour maps of isolated SiH_4 and BH_3 are also depicted to show how the electronic structure changes upon bonding.

The bonding nature of the $SiH_{4-n}X_n-BH_3$ complexes can further be quantified by three parameters[43,44] characterizing the BCP of the bridged bond and the terminal ones (Table 3). The first parameter is the electron density at BCP (ρ_c), reflecting the total charge accumulation at these points. Typically, the bridged B(Si)−H−B bond has a lower ρ_c than the terminal B−H bond. In the bridged Si−H−B bonds, the Si−H parts have a much lower ρ_c than the H−B parts. The second parameter is the Laplacian of ρ at a BCP ($\nabla^2\rho_c$), the curvature of gradient path at the BCP. This is a measure of covalent ($\nabla^2\rho_c < 0$) or ionic ($\nabla^2\rho_c > 0$) bonding nature. All of the terminal B−H bonds show negative $\nabla^2\rho_c$, and they are essentially covalent. The $\nabla^2\rho_c$ of bridged B−H is negative but near zero for B_2H_6, whereas it is positive for $B_2H_7^-$ and $SiH_{4-n}X_n-BH_3$. The ionic feature is more evident for the bridged B−H bond in $SiH_{4-n}X_n$−BH_3. The third parameter is the ellipticity (ϵ) at a BCP. For a BCP with a large ρ_c, ϵ is a measure of π character of the bond, whereas for a BCP with small ρ_c, ϵ is a measure of instability of the bond. The π character of the bridged B−H bond is more evident for B_2H_6 than for the other species. The large ϵ values for the bridged Si−H bonds indicate their relative instability. In summary, the $SiH_{4-n}X_n$−BH_3 complexes are bonded primarily by one bridged Si−H−B bond. Compared with B_2H_6 and $B_2H_7^-$, the Si−H−B bond is weaker and appears more ionic characteristics. Although only one Si−H−B bond is formed, some attractive nonbonding interaction between silicon and another hydrogen atom exist.

IV. Concluding Remarks

The $SiH_{4-n}X_n$−BH_3 complexes prefer the hydrogen-bridged structures to the halogen-bridged ones. The binding energies calculated at the MP2/aug-cc-pVTZ level are −6.43 to −12.06 with ZPE and BSSE corrections and −14.73 to −21.65 kcal/mol without the corrections. $SiH_{4-n}X_n$−BH_3 complexes show similar structures with mono-bridged anion $B_2H_7^-$, because one Si−H−B bond is definitely formed in all of the $SiH_{4-n}X_n$−BH_3 complexes according to the topological analysis of electron density based on the AIM theory. The geometry and electronic structures of the $SiH_{4-n}X_n$−BH_3 complexes also show characteristics of the double-bridged B_2H_6. The Si−H−B bond is polarized with the H closer to boron. The Si−H bonds are activated through bridging and thus may be the probable points of bond broken. The mechanisms of formation and subsequent fate of the $SiH_{4-n}X_n$−BH_3 complexes, however, require further investigation.

Acknowledgment. We thank Professor Kwang S. Kim, the director of the National Creative Research Initiative Center for Superfunctional Materials, Department of Chemistry, Division of Molecular and Life Sciences, Pohang University of Science and Technology, South Korea, for his kindly help and instructive discussions.

References and Notes

(1) Sasaoka, C.; Usui, A. *Appl. Surf. Sci.* **1994**, *82*, 348.
(2) Chung, C. H.; Han, J. H.; Rhee, S. W.; Moon, S. H. *Korean J. Chem. Eng.* **1995**, *12*, 593.
(3) Kitoh, H.; Muroyama, M.; Sasaki, M.; Iwasawa, M.; Kimura, H. *Jpn. J. Appl. Phys.* **1996**, *135*, 1464.
(4) Kongetira, P.; Neudeck, G. W.; Takoudis, C. G. *J. Vac. Sci. Technol. B* **1997**, *15*, 1902.
(5) Lengyel, I.; Jensen, K. F. *Thin Solid Films* **2000**, *365*, 231.
(6) Nishizawa, M.; Yasuda, T.; Yamasaki, S.; Shinohara, M.; Kamakura, N.; Kimura, Y.; Niwano, M. *J. Vac. Sci. Technol. A* **2001**, *19*, 2001.
(7) Walch, S. P.; Dateo, C. E. *J. Phys. Chem. A* **2001**, *105*, 2015.
(8) Perrin, J.; Takeda, Y.; Hirano, N.; Takeuchi, Y.; Matsuda, A. *Surf. Sci.* **1989**, *114*, 210.
(9) Das, D.; Sharma, S. N.; Bhattacharyya, T. K.; Chattopadhyay, Barua, S. A. K.; Banerjee, R. *Solid State Commun.* **1996**, *97*, 769.
(10) Briand, D.; Sarret, M.; Kis-Sion, K.; Mohammed-Brahim, T.; Duverneuil, P. *Semicond. Sci. Technol.* **1999**, *14*, 173.
(11) Pejnefors, J.; Zhang, S. L.; Radamson, H. H.; Grahn, J. V.; Ostling, M. *J. Appl. Phys.* **2000**, *88*, 1655.
(12) Payne, A. M.; Wagner, S. *Appl. Phys. Lett.* **2000**, *76*, 2949.
(13) Hay, P. J.; Boehm, R. C.; Kress, J. D.; Martin, R. L. *Surf. Sci.* **1999**, *436*, 175.
(14) Habuka, H.; Akiyama, S.; Otsuka, T.; Qu, W. F. *J. Cryst. Growth* **2000**, *209*, 807.
(15) Kamiya, T.; Maeda, Y.; Nakahata, K.; Komaru, T.; Fortmann, C. M.; Shimizu, I. *J. Ceram. Soc. Jpn.* **1999**, *107*, 1099.
(16) Yang, G.; Bai, P.; Tong, B. Y.; Wong, S. K.; Hill, I. *Solid State Commun.* **1989**, *72*, 159.
(17) Perrin, J.; Takeda, Y.; Takeuchi, Y. *Sur. Sci.* **1989**, *210*, 114.
(18) Hu, S.-W.; Kim, J.; Tarakeshwar, P.; Kim, K. S. *J. Phys. Chem. A* **2002**, *106*, 6817.
(19) Boys, S. F.; Bernardi, F. *Mol. Phys.* **1970**, *19*, 553.
(20) Frisch, M. J.; Trucks, G. W.; Schlegel, H. B.; Scuseria, G. E.; Robb, M. A.; Cheeseman, J. R.; Zakrzewski, V. G.; Montgomery, J. A., Jr.; Stratmann, R. E.; Burant, J. C.; Dapprich, S.; Millam, J. M.; Daniels, A. D.; Kudin, K. N.; Strain, M. C.; Farkas, O.; Tomasi, J.; Barone, V.; Cossi, M.; Cammi, R.; Mennucci, B.; Pomelli, C.; Adamo, C.; Clifford, S.; Ochterski, J.; Petersson, G. A.; Ayala, P. Y.; Cui, Q.; Morokuma, K.; Malick, D. K.; Rabuck, A. D.; Raghavachari, K.; Foresman, J. B.; Cioslowski, J.; Ortiz, J. V.; Stefanov, B. B.; Liu, G.; Liashenko, A.; Piskorz, P.; Komaromi, I.; Gomperts, R.; Martin, R. L.; Fox, D. J.; Keith, T.; Al-Laham, M. A.; Peng, C. Y.; Nanayakkara, A.; Gonzalez, C.; Challacombe, M.; Gill, P. M. W.; Johnson, B. G.; Chen, W.; Wong, M. W.; Andres, J. L.; Head-Gordon, M.; Replogle, E. S.; Pople, J. A. *Gaussian 98*, revision A.7; Gaussian, Inc.: Pittsburgh, PA, 1998.
(21) Biegler-Konig, F.; Schonbohm, J.; Bayles, D. *J. Comput. Chem.* **2001**, *22*, 545.
(22) Bader, R. F. W. *Atoms in Molecules: A Quantum Theory*; Oxford University Press: Oxford, U.K., 1990.
(23) Mo, Y. R.; Gao, J. L. *J. Phys. Chem. A* **2001**, *105*, 6530.
(24) Yumatov, V. D.; Il′inchik, E. A.; Mazalov, L. N.; Volkov, O. V.; Volkov, V. V. *J. Struct. Chem.* **2001**, *42*, 281.
(25) Sinke, E. J.; Pressley, G. A., Jr.; Baylis, A. B.; Stafford, F. E. *J. Chem. Phys.* **1964**, *41*, 2207.
(26) Burgaul, A. B.; Fu, V. C. *J. Am. Chem. Soc.* **1966**, *88*, 1147.
(27) Gangulin, P. S.; Mcgee, H. A. *J. Chem. Phys.* **1969**, *50*, 4658.
(28) Ahlrichs, R. *Theor. Chim. Acta* **1974**, *35*, 59.
(29) Evans, W. G.; Holloway, C. E.; Sukumarabundhu, K.; Mcdaniel, D. H. *Inorg. Chem.* **1968**, *7*, 1746.
(30) Shore, S. G.; Lawrence, S. H.; Watkins, M. I.; Bau, R. *J. Am. Chem. Soc.* **1982**, *104*, 7669.
(31) Raghavachari, K.; Schleyer, P. V. R.; Spitznagel, G. W. *J. Am. Chem. Soc.* **1983**, *105*, 5917.
(32) Thorne, L. R.; Suendram, R. D.; Lovas, F. J. *J. Chem. Phys.* **1983**, *78*, 167.
(33) Haaland, A. *Angew. Chem., Int. Ed. Engl.* **1989**, *28*, 992.
(34) Brint, P.; Sangchakr, B.; Fowler, P. W. *J. Chem. Soc., Faraday Trans.* **1989**, *85*, 29.
(35) Mckee, M. L. *J. Phys. Chem.* **1992**, *92*, 5380.
(36) Leboeuf, M.; Russo, N.; Salahub, D. R.; Toscano, M. *J. Chem. Phys.* **1995**, *103*, 7408.
(37) Dapprich, S.; Frenking, G. *J. Phys. Chem.* **1995**, *99*, 9352.
(38) Anane, H.; Boutalib, A.; Tomas, F. *J. Phys. Chem. A* **1997**, *101*, 7879.
(39) Cook, D. B.; Sordo, J. A.; Sordo, T. L. *Int. J. Quantum Chem.* **1993**, *48*, 375.
(40) Pudzianowski, A. T. *J. Chem. Phys.* **1995**, *102*, 8029.
(41) Lendvay, G.; Mayer, I. *Chem. Phys. Lett.* **1998**, *297*, 365.
(42) Kestner, N. R.; Combariza, J. E. In *Reviews in Computational Chemistry*; Lipkowitz, K. B., Boyd, D. B., Eds.; Wiley-VCH, Inc.: New York, 1999; Vol.13, Chapter 2.
(43) Popelier, P. L. A. *J. Phys. Chem. A* **1998**, *102*, 1873.
(44) Grabowski, S. J. *J. Phys. Chem. A* **2001**, *105*, 10739.